


## Nonlinear electromagnetic pulse isolator

A. A. Zabolotskii *Institute of Automation & Electrometry of Siberian Branch of the RAS, Academic Koptug ave.1, 690090 Novosibirsk, Russian Federation*

(Received 11 October 2019; revised manuscript received 7 March 2020; accepted 20 April 2020; published 18 May 2020)

A nonlinear medium with nonreciprocal propagation of electromagnetic field pulses is proposed and studied. The medium consists of a long waveguide surrounded by two-level media implanted in a straight spiral. Respective Maxwell-Bloch system describing evolution of the pulses in the waveguide with nonlinear feedback is derived. The influence of the neighbors' dipole fields taken into account in the tight bounding approximation manifests itself in the appearance of the nonlinear differential terms. Under the condition of unidirectional propagation of field pulses, the Maxwell-Bloch system of equations is reduced to an integrable system. Analysis of obtained exact solutions have shown that these differential terms are responsible for the nonreciprocity of the propagation of field pulses in the waveguide. Using the soliton solution as an example, it is shown that the spiral arrangement of atoms yields critical dependence of the evolution of field pulses on the direction of their propagation or on the chirality of the medium.

DOI: [10.1103/PhysRevA.101.053837](https://doi.org/10.1103/PhysRevA.101.053837)

### I. INTRODUCTION

The ability to control energy flows using nonlinear properties of physical systems is of both theoretical and important practical interest. Wave pulses can be controlled by creating a nonlinear isolator in which electromagnetic waves are transmitted differently for opposite directions of propagation. In a linear  $T$ -symmetric system, this possibility is forbidden by the reciprocity theorem [1]. Therefore, special attention is paid to the study of nonlinear media with nonreciprocal properties. In electromagnetics, nonreciprocity is now an important scientific and technological concept at both microwave and optical [2] frequencies; see review describing the current state of the problem [3]. Asymmetric wave propagation caused by nonlinearity arises in various fields of physics, including nonlinear optics. The so-called fully optical diode was predicted in [4–8], and then implemented experimentally in [9]. It is proposed to use the left-side metamaterials [10], quasiperiodic systems [11], coupled linear and nonlinear cavities [12–18], or  $PT$ -symmetric waveguides [1] as media for creating diodes or isolators. An electronic diode is a nonlinear semiconductor circuit component that allows conduction of electrical current in one direction only. A component with similar functionality for electromagnetic waves, an electromagnetic isolator [19], is based on the Faraday effect of rotation of the polarization state and is also a key component in optical and microwave systems [3]. In optics, the simplest isolator exploiting nonreciprocal transmission of circularly polarized light consists of a pair of polarizers and a Faraday rotator and it requires a static magnetic field [2]. A similar approach is also used for microwave devices. As another example, asymmetric transmission in metamaterial structures is allowed if propagation is accompanied by polarization conversion [6,8].

The most detailed analytical information about evolution of optical and other pulses may be obtained by solving an initial-boundary problem for completely integrable equations [20–22]. The first completely integrable Maxwell-Bloch equations describing electromagnetic wave evolution in a two-level system (TLS) had been derived by using the slow varying envelope approximation by Lamb [23]. Later, a set of integrable generalizations, which describe electromagnetic pulse evolution with and without application of the slow envelope approximation, had been derived [22]. Some of these models include the first and second derivatives of the TLS polarization [24].

If the distance between atoms is much less than the resonance wavelength, then the dipole-dipole interaction (DDI) can have a significant effect on the formation of localized excitations in dipole media and on many other linear and nonlinear processes. In two-dimensional and three-dimensional structures, for example, in magnets and liquid crystals, the effects associated with DDI and geometric factors play a critical role [25]. Optical chiral media with DDI can be formed on the basis of the spiral arrangement of resonant atoms; see, for example, Ref. [26]. Interfacing light with atoms localized near nanophotonic structures has attracted increasing attention in recent years. Exemplary experimental platforms include waveguides [27,29], nanofibers [28], and molecular waveguide [29].

The ultimate aim of the present work is to show that synergetic action of the chiral geometry of the DDI and nonlinear feedback yields violation of the reciprocity conditions for the propagation of optical solitons in a waveguide surrounded with atoms imbedded into spirals chains. Such an artificial nanosystem with coherent nonlinear feedback exhibits the properties of an electromagnetic pulse isolator (EMPI) for pulses without power limitation.

The paper is organized as follows. In the next section of this article, a basic system of evolution equations is derived that

\*zabolotskii@iae.nsk.su

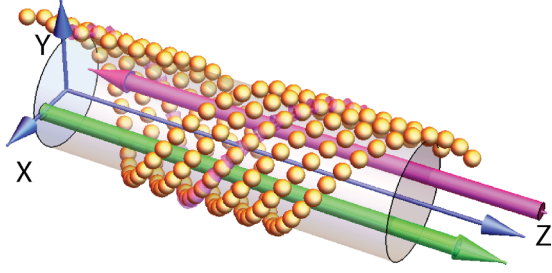


FIG. 1. Structure of the chiral system. The directions of propagation of field pulses in thin waveguide along and against the axis  $z$  are shown by red and blue arrows. Spheres show the TLSs embedded in spirals.

describes the dynamics of ultrashort electromagnetic pulses in a waveguide surrounded by helically arranged TLSs. In Sec. II the zero curvature presentation of derived reduced Maxwell-Bloch equations (RMBE) is derived. Soliton solutions are shown in Sec. III. In Sec. IV the obtained results and their applications are discussed. In the Appendix the ISTM apparatus associated with the system under consideration is presented.

## II. PHYSICAL ONSETS OF THE MODEL

Nonlinear asymmetric transmission can only occur in the presence of a strong intensity dependent propagation effect. The idea is to exploit the intensity dependence of the gyrotropy in chiral media, which manifests itself as differential circular birefringence and dichroism. The nonreciprocity phenomenon is often associated with chiral media. The simplest way to construct a chiral medium is to use straight, equally oriented spirals of the same chirality. The rotation of the polarization of the electromagnetic field propagating in the waveguide along the axes of the spirals in such a medium is determined by the interaction with the media dielectric constant, which describes the effects of gyrotropy and birefringence. If the spirals consist of nonlinear media, then for a sufficiently strong field feedback may occur, which will lead to an increase in the degree of nonreciprocity. Nonlinear nonreciprocal media with lossless coherent interaction are of particular interest. The scheme proposed here of a nonlinear nonreciprocal medium consisting of a long waveguide surrounded by helices with implanted TLS has such properties. This scheme is shown in Fig. 1, where it is assumed that atoms or molecules are described by TLS, which are implanted on curves forming spirals in the immediate vicinity of a long waveguide. The dipole moments of excited TLS transitions generate an electromagnetic field acting on the pulses propagating inside the waveguide. Note that, as helical chains, cyanine dyes can be used in the J-aggregates in the scheme under consideration. Such extended spiral molecular structures can be synthesized as a result of self-assembly [30]. The dipole moments of cyanine dyes that form long bunches in an aqueous solution [31,32] are of the order  $10^{-14}$  cgs.

Consider a chain of atoms placed on the curve  $\gamma(s)$ , where variable  $s$  is a point lying on the curve  $\gamma$  and  $s = s_n$  is the position of the  $n$ th TLS.  $s_n - s_{n-1}$  is the arc length between the closest neighbor TLSs. The interaction energy of the field

$\tilde{E}(s)$  with the polarization of the medium  $\tilde{P}(s) = \sum_n g_d(s - s_n) \tilde{\rho}(s_n)$  is proportional to  $-\tilde{E} \cdot \tilde{P}_m$ , where  $s_n = an$ ,  $n = \dots -2, -1, 0, 1, 2, \dots$  are the coordinates of the atoms on the curve,  $\tilde{\rho}$  is the induced polarization of one atom, and  $g_d$  is the interaction coefficient. The tilde sign above the functions means that they are defined at a point on the curve  $s \in \gamma(s)$ . The close arrangement of atoms leads to nonlocal interaction. To simplify the model, we use the approximation of nearest neighbors, which has been previously applied to similar molecular chains; see, for example, Refs. [33,34]. Note that here we consider a scale smaller than the wavelength, i.e., the dipole field decreases as a cube of distance, and ultrashort pulses, i.e., the excitation of sufficiently distant neighboring atoms can be neglected. In the approximation of the nearest neighbors, we obtain

$$\tilde{P}(s_n) \approx \tilde{\rho}(\gamma(s_n)) + g_d(s_n - s_{n-1}) \tilde{\rho}(\gamma(s_{n-1})) + g_d(s_n - s_{n+1}) \tilde{\rho}(\gamma(s_{n+1})), \quad (1)$$

where  $g_d(s_n - s_{n-1})$  is the coefficient of the interaction of the nearest-neighboring TLSs with dipole moments  $\vec{d}_n$  at the point  $s_n$ . This coefficient takes the form in the dipole-dipole approximation

$$g_d(s_n - s_{n-1}) = \frac{1}{4\pi\epsilon_0|\vec{n}|^3} \left[ \vec{d}_n \cdot \vec{d}_{n-1} - 3 \left( \frac{\vec{n}}{|\vec{n}|} \cdot \vec{d}_n \right) \left( \frac{\vec{n}}{|\vec{n}|} \cdot \vec{d}_{n-1} \right) \right], \quad (2)$$

where  $\vec{n}$  is a vector connecting points  $s_n$  and  $s_{n-1}$ ,  $\vec{d}_n$  is the vector of dipole moment of the TLS at the point  $s_n$ , and  $\epsilon_0$  is the dielectric susceptibility of the vacuum. It is assumed that  $|\vec{n}| = a$ ,  $|\vec{d}_n| = d \forall n$ . In the continuous approximation the vector  $\vec{n}$  is directed along the tangential vector. For an electromagnetic field with transverse polarization, the expression (2) is simplified:

$$g_d(s_n - s_{n-1}) = g_0 = \frac{d^2}{4\pi\epsilon_0 a^3}. \quad (3)$$

The effects due to the curvature of the chains described in the continuum limit by covariant derivatives are studied below.

The pulses of the field  $\tilde{E}$  propagate along and against the direction of the axis  $z$  in a waveguide inside the helical chains; see Fig. 1. In order to set up the appropriate tight-binding model describing the 1D motion of the field pulses along a waveguide, the 3D space helical structural properties of the system will be taken into account. In the Cartesian coordinates  $e_{x,y,z}$ , the spiral  $\gamma(s)$  has the form

$$\gamma(s) = \mathcal{R}[e_x \cos(\phi) + e_y \sin(\phi)] + e_z \mathcal{C} \phi \mathcal{P}, \quad (4)$$

where  $\phi = s/\mathcal{L}$ ,  $\mathcal{L} = \sqrt{\mathcal{P}^2 + \mathcal{R}^2}$ ,  $\mathcal{R}$  and  $\mathcal{P}$  are the radius and step of the spiral, respectively, and  $\mathcal{C} = \pm 1$  is the chirality of the spiral. For symmetrical helices considered here the curvature  $\mathcal{C}_h = \mathcal{R}/\mathcal{L}^2$ , as well as the torsion  $\mathcal{T}_h = \mathcal{C}\mathcal{P}/\mathcal{L}^2$ , are constants. We assume that  $s_n - s_{n-1} \ll \mathcal{R}, \mathcal{P}$ . The difference between the projections of the atomic positions in the spiral onto the longitudinal coordinate  $z$  has the form

$$z_n - z_{n-1} = (s_n - s_{n-1}) \mathcal{C}\mathcal{P}/\mathcal{L} \equiv a \mathcal{C}\mathcal{P}/\mathcal{L}. \quad (5)$$

The tangential  $\mathbf{T} = \partial_s \gamma(s)$ ; normal  $\mathbf{N}$  and binormal  $\mathbf{B}$  vectors form the Frenet-Serret basis [25]. In Cartesian coordinates, the

Frenet-Serret basis has the following representation:

$$\begin{bmatrix} \mathbf{T} \\ \mathbf{N} \\ \mathbf{B} \end{bmatrix} = \hat{M} \begin{bmatrix} \mathbf{e}_z \\ \mathbf{e}_x \\ \mathbf{e}_y \end{bmatrix} \\ \equiv \begin{bmatrix} -\mathcal{L}C_h \sin(\phi) & \mathcal{L}C_h \cos(\phi) & \mathcal{L}\mathcal{T}_h \\ -\cos(\phi) & -\sin(\phi) & 0 \\ \mathcal{L}\mathcal{T}_h \sin(\phi) & -\mathcal{L}\mathcal{T}_h \cos(\phi) & \mathcal{L}C_h \end{bmatrix} \begin{bmatrix} \mathbf{e}_z \\ \mathbf{e}_x \\ \mathbf{e}_y \end{bmatrix}. \quad (6)$$

Here I consider for simplicity a limiting case of  $C_h \rightarrow 0$ . Then transform (6) reduces to the rotation of the normal and binormal vectors around the  $z$  axis. To take into account the influence of the fields of induced dipoles of neighboring atoms, we turn to the rotating coordinate system  $\tilde{\mathbf{p}} = \hat{M}(C_h \rightarrow 0)\mathbf{P}$ ,  $\tilde{\mathbf{E}} = \hat{M}(C_h \rightarrow 0)\mathbf{E}$ , where  $\mathbf{P} = \{P_x, P_y, P_z\}^T$ ,  $\mathbf{E} = \{E_x, E_y, E_z\}^T$ . Here functions without a tilde on them are defined on the line  $z$ . When shifted by  $s \rightarrow s \pm a$ , the vector of polarization  $\mathbf{P}_\perp = \{P_x, P_y\}^T$  changes as  $\mathbf{P}_\perp(s) \rightarrow \hat{M}_\perp(s)^{-1} \hat{M}_\perp(s \pm a) \mathbf{P}_\perp(s \pm a) = \hat{M}_\perp(\pm a) \mathbf{P}_\perp(s \pm a)$ . In contrast to a rectilinear medium, a shift by  $\pm a$  is accompanied here by the rotation, which is described by the matrix  $\hat{M}_\perp(\pm a)$ , where

$$\hat{M}_\perp(s) = \begin{bmatrix} -\cos(\phi) & -\sin(\phi) \\ \sin(\phi) & -\cos(\phi) \end{bmatrix}. \quad (7)$$

Using this property, we find from (1) taking into account the projection onto axis  $z$

$$\begin{aligned} & \hat{M}_\perp(a) \mathbf{P}_\perp(s+a) + \hat{M}_\perp(-a) \mathbf{P}_\perp(s-a) \\ &= 2\hat{\mathbb{I}} \mathbf{P}_\perp(s) - 2a^2 \mathcal{T}_h \begin{bmatrix} 0 & 1 \\ -1 & 0 \end{bmatrix} \partial_z \mathbf{P}_\perp(z) \\ &+ a^2 \hat{\mathbb{I}} \partial_z^2 \mathbf{P}_\perp(s) + \mathcal{O}(a^3), \end{aligned} \quad (8)$$

where  $\hat{\mathbb{I}}$  is the unit  $2 \times 2$  matrix. In the second term in the right-hand side of Eq. (8) the projection to the  $z$  axis is used with taking into account relation (5).

The integrability of the model allows one to reveal the determining nonlinear effects, analyze the role of the initial conditions, and compare with the results of numerical analysis of the more general model. To find a completely integrable model the standard conditions, such as the absence of losses and a one-dimensional approximation, have been used. Additionally, the curvature of the spiral and the second derivative with respect to  $s$  on the right side of (8) have been neglected. For  $C_h = 0$  and under proposition that medium does not have intrinsic biaxial anisotropy the projection of the field onto  $z$  axis can be set equal to zero. In the tight coupling approximation, taking into account the fields of the nearest neighbors, the Maxwell equations describing the evolution of a two-component electric field in a rectilinear waveguide propagating in or against the direction of the  $z$  axis (see Fig. 1) have the form

$$\begin{aligned} & \left[ \partial_z^2 - \frac{1}{c^2} \partial_t^2 \right] \mathbf{E}_\perp \\ &= \frac{4\pi N_a d_a}{c^2} \partial_t^2 \left[ (1 + 2g_0) + \gamma_c \begin{pmatrix} 0 & 1 \\ -1 & 0 \end{pmatrix} \partial_z \right] \mathbf{P}_\perp. \end{aligned} \quad (9)$$

Here  $g_0 = g_d(\pm a)$ , see Eq. (3),  $\gamma_c = -g_0 2a^2 \mathcal{C} \mathcal{P} / \mathcal{L}$ ,  $c$  is the light velocity, and  $\mathbf{E}_\perp = \{E_x(z, t), E_y(z, t)\}^T$ . The matrix term in the right-hand side of Eq. (9) with the coefficient  $\gamma_c$  is due to the influence of the curvilinear arrangement of atoms around the waveguide.

For  $4\pi N_a d_a^2 / \hbar \omega_a \leq 1$ , where  $N_a, d_a, \omega_a$  are the density of the TLSs, the dipole moment, and transition frequency, respectively, the unidirectional propagation approximation of light pulses is applicable in an extended one-dimensional medium [35]. In most two-level media for the characteristic values of dipole moments used in experiments, the unidirectional propagation approximation is possible at a sufficiently high density of  $N_a \sim 10^{-18} \text{ cm}^{-3}$ . The unidirectional propagation approximation meets the formal conditions:

$$\partial_z + \epsilon \partial_{ct} \ll \partial_t, \partial_z, \quad (10)$$

where  $\epsilon = 1$  corresponds to the field propagation direction from  $z = -\infty$  to  $z = \infty$ , and  $\epsilon = -1$  corresponds to the opposite direction. Then using (10) we present the left-hand side of Eq. (9) as

$$\begin{aligned} & \left[ \partial_z^2 - \frac{1}{c^2} \partial_t^2 \right] \frac{E_{x,y} c^2}{4\pi N_a d_a^2 (1 + 2g_0)} \\ &= \left[ \partial_z + \frac{\epsilon}{c} \partial_t \right] \left[ \partial_z - \frac{\epsilon}{c} \partial_t \right] \frac{E_{x,y} \hbar c^2}{4\pi N_a d_a^2 \omega (1 + 2g_0)} \\ &\approx -2\partial_t \partial_\chi E_{x,y}, \end{aligned} \quad (11)$$

where  $E_{x,y} = d_0 \mathcal{E}_{x,y} / (\hbar \omega)$  is the dimensionless amplitude and

$$\chi = \frac{4\pi N_a d_a^2 \omega_0 (1 + 2g_0)}{\hbar c^2} (\epsilon z - ct). \quad (12)$$

Under the conditions (10), Eq. (9) takes the form

$$\frac{\partial E_x}{\partial \chi} = q \frac{\partial P_x}{\partial \varsigma} + b \frac{\partial^2 P_y}{\partial \varsigma^2}, \quad (13)$$

$$\frac{\partial E_y}{\partial \chi} = q \frac{\partial P_y}{\partial \varsigma} - b \frac{\partial^2 P_x}{\partial \varsigma^2}, \quad (14)$$

where  $q = -1$ ,  $\varsigma = t\omega$ ,  $\epsilon = \epsilon \mathcal{C}$ , and

$$b = \frac{-\epsilon g_0 \omega}{(1 + 2g_0) \mathcal{L} c}. \quad (15)$$

Given the dimensionless normalization of time variable and the components of the field amplitude, let us represent the Bloch equations for a two-level medium in the form

$$\partial_\varsigma P_x = -P_y + E_y S_z, \quad (16)$$

$$\partial_\varsigma P_y = P_x - E_x S_z, \quad (17)$$

$$\partial_\varsigma S_z = E_x P_y - E_y P_x, \quad (18)$$

where  $S_z$  is the normalized difference of the levels populations [36]. Note that the equations (16)–(18) are invariant with respect to the rotation described by the matrix (7). Rewrite Eqs. (13), (14), and (16)–(18) as

$$\frac{\partial E}{\partial \chi} = q \frac{\partial S}{\partial \varsigma} - ib \frac{\partial^2 S}{\partial \varsigma^2}, \quad (19)$$

$$\partial_\varsigma S = iS - iE S_z, \quad (20)$$

$$\partial_{\zeta} S_z = \frac{i}{2}(ES^* - E^*S), \quad (21)$$

where  $E = E_x + iE_y$  and  $S = P_x + iP_y$ .

For the dipole field  $g_0 < 0$  and supposing that  $1 + 2g_0 > 0$ , I put  $b = \varepsilon|b|$ , since  $\varepsilon = \pm 1$ . The RMBE (19)–(21) are the compatibility conditions for the following linear systems:

$$\partial_{\zeta} \psi = \begin{bmatrix} -i\lambda & \gamma_x E \\ \tilde{\gamma}_x E^* & i\lambda \end{bmatrix} \psi, \quad (22)$$

$$\partial_{\chi} \psi = \begin{bmatrix} i \frac{\lambda(2b\lambda - q)}{2\lambda + 1} S_z & \gamma_x \left[ \frac{b+q}{2\lambda+1} S - bES_z \right] \\ \tilde{\gamma}_x \left[ \frac{b+q}{2\lambda+1} S^* - bE^*S_z \right] & -i \frac{\lambda(2b\lambda - q)}{2\lambda + 1} S_z \end{bmatrix} \psi, \quad (23)$$

where  $\gamma_x = \varepsilon\lambda\sqrt{|b|}$  and  $\tilde{\gamma}_x = -[\lambda - q/(2b)]\sqrt{|b|}$ .

### III. SOLITON SOLUTION

To demonstrate the features of the optical diode mechanism, we study the properties of the soliton solution of the system (19)–(21) for different  $\varepsilon$ . The right side of the equation (19) describes the source that supports the pulse of the field having the soliton form propagating in the waveguide. To find soliton solutions, we reduce the spectral problem (SP) (22) to one previously studied in application of the inverse scattering transform to other physical models. For this aim, let us denote  $\lambda = \eta + f$ ,  $f = q/(4b)$ , and  $G = \sqrt{|b|}E e^{i2f\zeta}$ . Replace  $\psi = \Psi e^{-i\sigma_3 f\zeta}$  ( $\sigma_3$  is the Pauli matrix). Then introduce the functions  $F(\tau)$  such that  $G = F(\tau)/F_3(\tau)$  and  $\tau$  as a new variable by the relation  $d\zeta = F_3(\tau)d\tau$ , where  $F_3 = \sqrt{1 - \varepsilon|F|^2}$ . Then the SP (22) transforms to the following form:

$$\partial_{\tau} \Psi = \begin{bmatrix} -i\eta F_3 & \varepsilon(\eta + f)F \\ -(\eta - f)F^* & i\eta F_3 \end{bmatrix} \Psi. \quad (24)$$

The linear system (24) had been studied, for instance, in [37]. Respective apparatus developed for analogous SP can be used for constructing soliton solutions. SPs close to (24) were used to solve the equations of the chiral field, two- and four-wave interaction, and Landau-Lifshitz equations; see, for example, in [24,37–41].

Effect of the nonreciprocal propagation may be demonstrated on the simplest, but nontrivial soliton solution. For initial boundary data,  $E_{\pm\infty} = 0$ ,  $\chi = 0$ ,  $S_z(\chi) = -1$ ,  $P(\chi) = 0$ , we find the functions  $F_3, F$  defying soliton solution; see, for details, in the Appendix,

$$F_3(\tau, \chi) = \frac{|\cosh(\theta + i\delta)|^2 - \varepsilon\kappa^2}{|\cosh(\theta + i\delta)|^2 + \varepsilon\kappa^2}, \quad (25)$$

$$F(\tau, \chi) = \frac{2\kappa \cosh(\theta + i\delta)e^{2i\theta_2}}{|\cosh(\theta + i\delta)|^2 + \varepsilon\kappa^2}, \quad (26)$$

where  $\theta = \theta_1 + i\theta_2$ ,

$$\theta_1 = 2 \operatorname{Im}(\eta)[\tau - bw_0(\chi - \chi_1)], \quad (27)$$

$$\theta_2 = -\frac{2b - q}{2}w_0(\chi - \chi_2), \quad (28)$$

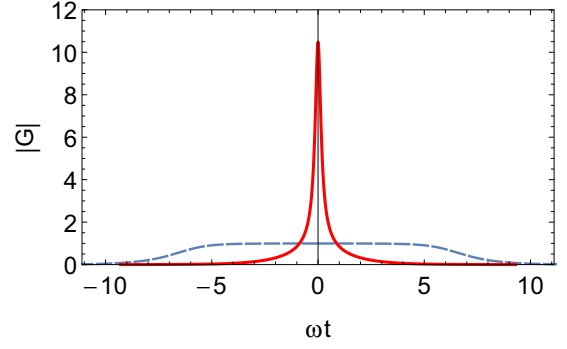


FIG. 2. Pulse shapes of the fields  $|G(\zeta)|$  propagating along ( $\varepsilon = 1$ ) the axis  $z$  and in the opposite direction ( $\varepsilon = -1$ ) are shown by solid and dashed lines, respectively, for  $\eta_1 = 0.4$ ,  $|q/b| = 1.5$ ,  $\mathcal{C} = 1$ . Units are dimensionless. Estimation of the physical quantities yields as follows. For the wavelength  $5 \mu\text{m}$  the pulse energy is  $100 \mu\text{J}$  ( $|G|^2 \sim 1.5 \times 10^2$ ) and the power pulse duration is about 100 fs corresponding to  $\omega t \sim 6$ .

$$\frac{f + \eta^*}{f + \eta} = e^{-2i\delta}, \quad \kappa = \frac{\operatorname{Im}(\eta)}{|f + \eta|}, \quad (29)$$

and  $\chi_{1,2}$  are some constants determined from the initial conditions. For  $\eta = i\eta_1$ ,  $\eta_1 \in \mathbb{R}$  one gets  $w_0(\eta_1) = (16b^2\eta_1^2 + q^2)/[16b^2\eta_1^2 + (q - 2b)^2]$ .

The function  $\tau(t)$  is found implicitly by integrating the equality  $F_3(\tau)d\tau = d\omega t$ ,

$$A \arctan \left\{ \frac{\sqrt{2}[\cos(2\delta) + 2\varepsilon\kappa^2 - 1] \tanh[2\eta_1(\tau - \tau_0)]}{\sqrt{1 - 8\varepsilon\kappa^2 \cos(2\delta) - \cos(4\delta) - 8\kappa^4}} \right\} + \tau = \omega t. \quad (30)$$

Here  $A = \sqrt{8\varepsilon\kappa^2}/\eta_1$ ,  $\tau_0 = bw_0(\chi - \chi_1)$ .

The time dependence of the soliton amplitude  $|G(t)| = |F|/F_3$  is shown in Fig. 2. The amplitude of the field momentum critically depends on the sign of  $\varepsilon$ , that is, either on the direction of propagation or on the chirality  $\mathcal{C}$ , as it is shown in Fig. 2. The ratio of these amplitudes increases with the simultaneous growth of  $\eta_1$  and  $|f|$  and decreases with increasing  $|f - \eta_1|$ . For  $\eta_1 \sim 1$  and increasing  $|b|$  nonlinear interaction in the chiral medium leads to the formation of ultrashort pulses or low amplitude pulses in dependence of the direction of propagation. Due to the geometrical and nonlinear effects pulse propagating along in the waveguide along  $z$  axis takes the form of an ultrashort pulse for  $\varepsilon = 1$ . The same effects under the same initial conditions and parameters lead to formation of the long pulse with the low amplitude propagating in the opposite direction ( $\varepsilon = -1$ ).

Let for definite the chirality  $\mathcal{C} = 1$ . The ratio of the amplitudes of solitons propagating in opposite directions  $T$  depends on the values of  $|b|$ ; see Eq. (14). Figure 3 shows the growth of  $T$  at  $\eta \rightarrow f$ . Unlike the nonlinear media considered in the works of [13,15], interaction with the TLS chain leads to strong feedback, which increases with increasing amplitude. It should be noted that the same but more strong dependence is manifested for  $\eta_1 > 1$ .



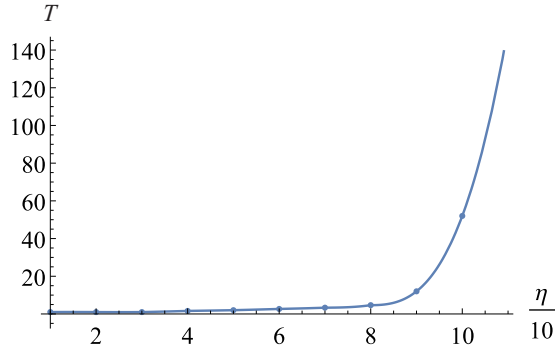


FIG. 3. Numerical results. The ratio of the amplitudes of solitons propagating to the right and to the left  $T$  vs the amplitude  $\eta$  for  $b = 1/4.4$ .

#### IV. DISCUSSION AND CONCLUSION

The integrable RMBE (19)–(21) describe the nonreciprocal propagation of electromagnetic pulses in a nonlinear medium and are derived by using the unidirectional propagation approximation. This approximation makes it possible to use the RMBE for modeling the properties of micro- and nanoscale EMPI operating beyond the slow envelope approximation. Spatial anisotropy in the system shown in Fig. 1 arising due to the chiral arrangement of the TLSs around the waveguide plays a critical role. The nonreciprocal propagation effect arises due to the local anisotropy and interaction of the field pulse with the induced polarization of the TLSs. Note the difference from the two-level medium models in which the quasistatic approximation is used and the contribution of polarizations are taken into account by introducing a local Lorentz field; see, for example, in Ref. [42]. In these cases the Lorentz field is the result of averaging over sizes much larger than the distance between atoms.

In deriving the RMBE to preserve complete integrability, the second-order dispersion (SOD) terms in the right-hand sides of Eq. (8) ( $\propto \partial_z^2 \mathbf{P}_\perp$ ) have been neglected. These terms arise due to the DDI in the tight coupling approximation. The SOD terms can be neglected provided that  $\partial_z \ll 2T_h$  or for  $2\lambda_{\text{light}} \gg \mathcal{L}$ , where  $\lambda_{\text{light}}$  is the wavelength of light corresponding to the transition energy of the TLS. The last inequality means that the number of spiral rings located at a wavelength distance is larger than unity. Numerical study shows that the SOD broadens the form of pulses. The change in the shape of the pulse with an increase in the ratio  $\gamma = T_h/\lambda_{\text{light}}$  is shown in Fig. 4 (see also Fig. 5).  $\gamma^{-1}$  is proportional to the effective number of full helical turns of a spiral at a wavelength. For nonsingular regime SOD equally reduces the amplitudes of pulses of the same shape, propagating in both directions, i.e., the ratio of their amplitudes does not change. At the same time for parameter values  $\eta \rightarrow f$  the shape of the field pulse tends to singular; see Fig. 3. With an increase in the amplitude and steepness of the pulse front, the influence of the SOD increases. More detailed study of the contributions of the SOD and other terms violating integrability requires further numerical investigation.

The geometry similar to that considered in this paper was used to observe Berry's topological phase in Ref. [16]. The key element in the experiment was a single-mode, helically

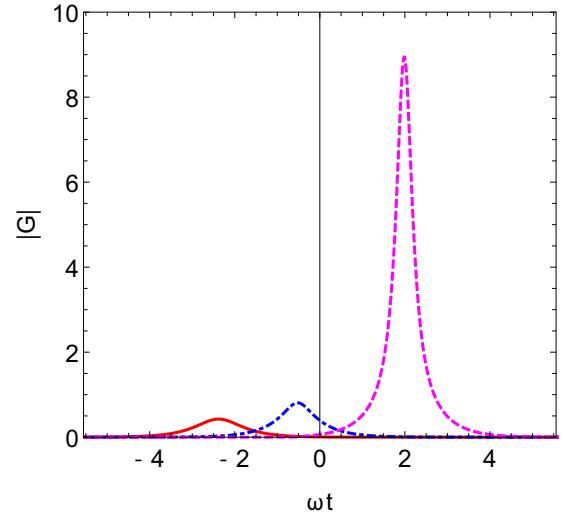


FIG. 4. Dependence of the form of the soliton on parameter  $b$ , obtained by analyzing the solution. The field intensity  $|G(\zeta = \omega t)|^2$  for  $1/|b| = 20, 12, 6$  are shown by solid (red), dot-dashed (blue), and dotted (magenta) lines, respectively. Parameters are  $\eta_1 = 1$ ,  $\mathcal{C} = 1$ . Units are dimensionless.

wound optical fiber, inside which a photon of a given helicity could be adiabatically transported around a closed path in momentum space. As in the present work, the photon polarization is controlled by the spiral structure of the surrounding waveguide. However, in contrast to Tomita's work [16], in the RMBE (19)–(21) nonlinear feedback plays a critical role. The field in the waveguide causes a change in the populations of the TLS levels and the induced dipole moments of the transitions, whose local fields in turn alter the polarization and amplitude of the field in a waveguide. As a result, the field acquires a nonlinear phase, which may be treated as analog of the Berry phase. The influence of this nonlinear phase is manifested in the appearance of a force, which for some parameter values suppresses the propagation of the pulse in one of the directions.

The authors of Ref. [17] have demonstrated polarization-dependent optical elements based on the Pancharatnam-Berry phase. The constructed elements are based on geometric phase modification resulting from space-variant polarization manipulation. The scheme shown in Fig. 1 considered here can be treated in a similar way if one considers the scattering of the field in a waveguide by a “frozen” excitation of a TLS in the spirals. Determining the form of frozen excitation requires an investigation of solutions to the inverse problem.

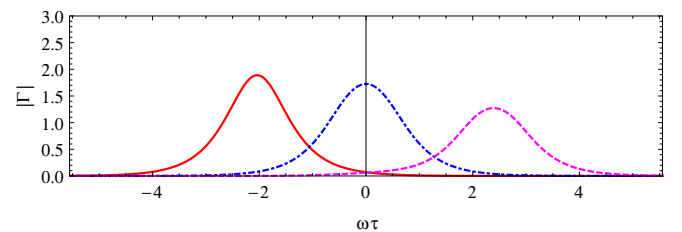


FIG. 5. Same as in Fig. 4 except that the pulse propagates in the opposite direction, i.e.,  $\mathcal{C} = -1$ .

Topological insulators are predicted for an electromagnetic wave. Substantial effort has been directed towards realizing topological insulators for electromagnetic waves; see citations in Ref. [18]. This is in the spirit of the proposed Floquet topological insulators, in which temporal variations in solid-state systems induce topological edge states. The authors of Ref. [18] have proposed and experimentally demonstrated a photonic topological insulator as a photonic lattice exhibiting topologically protected transport of visible light on the lattice edges. The scheme shown in Fig. 1 may be used as an element to form an array of evanescently coupled helical waveguides. However, taking into account the effects associated with the periodicity of the system for a nonlinear medium seems too complicated and cumbersome for analysis. Therefore, the completely integrable model derived in this work, which allows one to study the strongly nonlinear interaction stage leading to nonreciprocity, is of particular interest.

In Ref. [3], a classification of nonreciprocal systems is given. According to this classification, the model derived here corresponds to time-reversal symmetric breaking by spatial asymmetry and nonlinear self-biasing; see Chap. XXL in [3]. However, in contrast, the RMBE (19)–(21) has a number of fundamental differences from those described in review [3]. (I) There is no restriction on excitations and intensity. For large amplitudes of pulses, the nonreciprocity effect is more pronounced. (II) There is no restriction on excitation in only one direction. (III) There are no restrictions on the generation of harmonics. (IV) The interaction is purely coherent, that is, there are no losses in the system.

In the system shown in Fig. 1, along with the violation of spatial symmetry, there is a nonlinear feedback due to the coherent interaction of the polarization of the wave with the TLS transition. This feedback interaction leads to a nonlinear rotation of the polarization in the same or opposite direction, which occurs in the linear limit. This rotation is described by the gradient off-diagonal term on the right side of Eq. (19). This mechanism differs from that of known models of nonreciprocal nonlinear media. The proposed model with strong nonlinearity can be considered as an alternative to the known nonlinear models with weak nonlinearity, considered, for instance, in Refs. [13,15].

Note, finally, that the soliton solution of RMBE (19)–(21) demonstrates a qualitative change in the form and parameters of the soliton when the sign  $\varepsilon$  or the sign  $\mathcal{C}$  changes. The physical mechanism of action of EMPI is based on the interaction of induced dipoles in a medium with torsion  $\mathcal{T}_h \neq 0$ . Formally, a change in sign of  $\varepsilon$  corresponds to a change in the direction

of the charge current, which is described by the second term on the right side of Eq. (19). The signs  $\varepsilon \pm 1$  correspond to integrable models with different symmetry properties of the solutions of the spectral problem (24). As a consequence, the evolution of the forward and backward waves is described by systems of nonlinear equations with different properties. Generalization of the derived model paves the way to the investigation of a family of nonlinear waves featuring a strong interaction between the chiral chains of the TLSs and polarization of the electromagnetic pulses.

## ACKNOWLEDGMENTS

This work was supported by the Russian Foundation for Basic Research, Grant No. 18-02-00379, and the Ministry of Science and Higher Education of the Russian Federation, Grant No. AAAA-A17-117060810014-9.

## APPENDIX: ISTM EQUATIONS

Application of the technique of the inverse scattering transform to the SP (24) follows a well-known approach; see, for instance, in [38,39]. The solutions of the spectral problem (14) in the main text have the involution

$$\Phi = \mathbf{M}\Phi(\lambda^*)^* \mathbf{M}^{-1}, \quad (\text{A1})$$

where

$$\mathbf{M} = \begin{pmatrix} 0 & \varepsilon \frac{\lambda+f}{f-\lambda} \\ 1 & 0 \end{pmatrix}. \quad (\text{A2})$$

The respective Jost functions  $\Phi_{1,2}$  corresponded to decaying as  $\tau \rightarrow \pm\infty$  potential and its derivatives for ground state  $F_3(\varsigma) = 1, F(\varsigma) = 0$  possess the following asymptotics:

$$\Phi = \exp(-i\lambda\sigma_3\varsigma), \quad \tau \rightarrow \pm\infty. \quad (\text{A3})$$

The symmetry properties (A1) correspond to the following respective matrix forms of the Jost functions:

$$\Phi = \begin{pmatrix} \psi_1^\pm & \varepsilon \psi_2^{\pm*} \frac{\lambda+f}{f-\lambda} \\ \psi_2^\pm & \psi_1^{\pm*} \end{pmatrix}. \quad (\text{A4})$$

Respective functions are related by the scattering matrices  $\hat{\mathcal{S}}$

$$\Phi^- = \Phi^+ \hat{\mathcal{S}}, \quad (\text{A5})$$

where

$$\hat{\mathcal{S}} = \begin{pmatrix} a & b^* \\ -\varepsilon b(\lambda-f)/(\lambda+f) & a^* \end{pmatrix}. \quad (\text{A6})$$

The Jost functions have the presentation

$$\Phi^+(\varsigma) = e^{-i\lambda\sigma_3\varsigma} + \int_{\theta}^{\infty} \begin{pmatrix} \lambda K(\varsigma, s) & \varepsilon(\lambda+f)Q^*(\varsigma, s) \\ (\lambda-f)Q(\varsigma, s) & \lambda K^*(\varsigma, s) \end{pmatrix} e^{-i\lambda\sigma_3 s} ds. \quad (\text{A7})$$

Using these presentations of the Jost functions we derive from the spectral problem (14) in the main text and (A3)

$$F = \frac{2[1 - iK(\varsigma, \varsigma)]Q^*(\varsigma, \varsigma)}{[1 - iK(\varsigma, \varsigma)][1 + iK^*(\varsigma, \varsigma)] + \varepsilon|Q(\varsigma, \varsigma)|^2}, \quad (\text{A8})$$

$$F_3 = \frac{[1 - iK(\varsigma, \varsigma)][1 + iK^*(\varsigma, \varsigma)] - \varepsilon|Q(\varsigma, \varsigma)|^2}{[1 - iK(\varsigma, \varsigma)][1 + iK^*(\varsigma, \varsigma)] + \varepsilon|Q(\varsigma, \varsigma)|^2}. \quad (\text{A9})$$

The Marchenko-type equations are

$$\begin{aligned} & \varepsilon(f - i\partial_y)Q(\varsigma, y) + \mathcal{G}(\varsigma + y) \\ &= \int_{\varsigma}^{\infty} K^*(\varsigma, s)i\partial_y \mathcal{G}(s + y)ds, \end{aligned} \quad (\text{A10})$$

$$i\partial_y K(\varsigma, y) = - \int_{\varsigma}^{\infty} Q^*(\varsigma, s)(f + i\partial_y)\mathcal{G}(s + y)ds, \quad (\text{A11})$$

where

$$\mathcal{G}(y) = \int_{\mathcal{U}} \frac{b(\chi)e^{i\lambda y}}{a} \frac{d\lambda}{2\pi i}. \quad (\text{A12})$$

$\mathcal{U}$  is the contour of integration in the upper half-plane.

The scattering data dependence vs  $\chi$  for  $S_3(\chi, \varsigma) = S_0, S(\chi, \varsigma) = 0, \varsigma \rightarrow \pm\infty$  is determined by function

$$b(\chi) = b(0) \exp \left\{ iS_0 \left[ \frac{(bq + 4\eta)[(b^2 - 2)q + 4b\eta]}{2(bq + 4\eta + 2)} \right] \right\}. \quad (\text{A13})$$

Here  $\eta$  is a complex number in the upper half-plane. For one pole  $\eta_1$  one may rewrite  $b(\eta_1)/\partial_{\eta}a(\eta \rightarrow \eta_1) = e^{\chi_1 + i\chi_2}$ .

- 
- [1] V. N. Konotop, J. Yang, and D. A. Zezyulin, Nonlinear waves in PT-symmetric systems, *Rev. Mod. Phys.* **88**, 035002 (2016).
- [2] B. E. A. Saleh and M. C. Teich, *Fundamentals of Photonics*, 2nd ed. (Wiley-Interscience, New York, 2007).
- [3] C. Caloz, A. Alú, S. Tretyakov, D. Sounas, K. Achouri, and Z.-L. Deck-Léger, Electromagnetic Nonreciprocity, *Phys. Rev. Applied* **10**, 047001 (2018).
- [4] M. Scalora, J. P. Dowling, C. M. Bowden, and M. J. Bloemer, Optical limiting and switching of ultrashort pulses in nonlinear photonic band gap materials, *J. Appl. Phys.* **76**, 2023 (1994).
- [5] M. D. Tocci, M. J. Bloemer, M. Scalora, J. P. Dowling, and C. M. Bowden, Thin-film nonlinear optical diode, *Appl. Phys. Lett.* **66**, 2324 (1995).
- [6] V. A. Fedotov, P. L. Mladyonov, S. L. Prosvirnin, A. V. Rogacheva, Y. Chen, and N. I. Zheludev, Asymmetric Propagation of Electromagnetic Waves through a Planar Chiral Structure, *Phys. Rev. Lett.* **97**, 167401 (2006).
- [7] I. V. Shadrivov, V. A. Fedotov, D. Powell, Y. S. Kivshar, and N. I. Zheludev, Electromagnetic wave analog of an electronic diode, *New J. Phys.* **13**, 033025 (2011).
- [8] C. Menzel, C. Helgert, C. Rockstuhl, E.-B. Kley, A. Tünnermann, T. Pertsch, and F. Lederer, Asymmetric Transmission of Linearly Polarized Light at Optical Metamaterials, *Phys. Rev. Lett.* **104**, 253902 (2010).
- [9] K. Gallo, G. Assanto, K. R. Parameswaran, and M. M. Fejer, All-optical diode in a periodically poled lithium niobate waveguide, *Appl. Phys. Lett.* **79**, 314 (2001).
- [10] M. W. Feise, I. V. Shadrivov, and Y. S. Kivshar, Complete band gaps in one-dimensional left-handed periodic structures, *Phys. Rev. E* **71**, 037602 (2005).
- [11] F. Biancalana, All-optical diode action with quasiperiodic photonic crystals, *J. Appl. Phys.* **104**, 093113 (2008).
- [12] M. Krause, H. Renner, and E. Brinkmeyer, Optical isolation in silicon waveguides based on nonreciprocal Raman amplification, *Electron. Lett.* **44**, 691 (2008).
- [13] V. Grigoriev and F. Biancalana, Nonreciprocal switching thresholds in coupled nonlinear microcavities, *Opt. Lett.* **36**, 2131 (2011).
- [14] C. G. Poulton, R. Pant, A. Byrnes, S. Fan, M. J. Steel, and B. J. Eggleton, Design for broadband on-chip isolator using stimulated Brillouin scattering in dispersion-engineered chalcogenide waveguides, *Opt. Express* **20**, 21235 (2012).
- [15] Y. Shi, Z. Yu, and S. Fan, Limitations of nonlinear optical isolators due to dynamic reciprocity, *Nat. Photon.* **9**, 388 (2015).
- [16] A. Tomita and R. Y. Chiao, Observation of Berry's Topological Phase by Use of an Optical Fiber, *Phys. Rev. Lett.* **57**, 937 (1986).
- [17] Z. Bomzon, G. Biener, V. Kleiner, and E. Hasman, Space-variant Pancharatnam-Berry phase optical elements with computer generated subwavelength gratings, *Opt. Lett.* **27**, 1141 (2002).
- [18] M. Rechtsman, J. Zeuner, Y. Plotnik *et al.*, Photonic Floquet topological insulators, *Nature (London)* **496**, 196 (2013).
- [19] D. Jalas, A. Petrov, M. Eich *et al.*, What is-and what is not-an optical isolator, *Nat. Photon.* **7**, 579 (2013).
- [20] S. P. Novikov, S. V. Manakov, L. P. Pitaevskii, and V. E. Zakharov, *Theory of Solitons: The Inverse Scattering Method* (Springer-Verlag, Berlin, 1984).
- [21] A. I. Maimistov and A. M. Basharov, *Nonlinear Optical Waves* (Kluwer Academic Publisher, Dordrecht, 1999).
- [22] A. A. Zabolotskii, Integrable equations of a few cycle optical pulse propagation, *Eur. Phys. J. Spec. Top.* **173**, 193 (2009).
- [23] G. L. Lamb, Jr., Analytical descriptions of ultrashort optical pulse propagation in a resonant medium, *Rev. Mod. Phys.* **43**, 99 (1971).
- [24] A. A. Zabolotskii, Coherent pulse interaction with two-level system embedded in a dispersive medium, *Phys. Rev. A* **85**, 063833 (2012).
- [25] S. Sternberg, *Curvature in Mathematics and Physics* (Dover Publications, Inc., Mineola, NY, 2012).
- [26] A. A. Zabolotskii, Exciton dynamics in a helical molecular aggregate, *JETP* **127**, 448 (2018).
- [27] J. D. Thompson, T. G. Tiecke, N. P. de Leon, J. Feist, A. V. Akimov, M. Gullans, A. S. Zibrov, V. Vuletić, and M. D. Lukin, Coupling a single trapped atom to a nanoscale optical cavity, *Science* **340**, 1202 (2013).
- [28] D. E. Chang, V. Vuletić, and M. D. Lukin, Quantum nonlinear optics – photon by photon, *Nat. Photon.* **8**, 685 (2014).
- [29] A. A. Zabolotskii, Control of excitons in a bent bunch of molecular aggregates by dipole-dipole interaction with quantum dots, *JETP* **125**, 572 (2017).
- [30] F. Wurthner, T. E. Kaiser, and Ch. R. Saha-Muller, J-aggregates: From serendipitous discovery to supramolecular engineering of functional dye materials, *Angew. Chem., Int. Ed.* **50**, 3376 (2011).
- [31] A. V. Sorokin, A. A. Zabolotskii, N. V. Pereverzev, S. L. Yefimova, Y. V. Malyukin, and A. I. Plekhanov, Plasmon controlled exciton fluorescence of molecular aggregates, *J. Phys. Chem. C* **118**, 7599 (2014).
- [32] A. V. Sorokin, A. A. Zabolotskii, N. V. Pereverzev, I. I. Bepalova, S. L. Yefimova, Y. V. Malyukin, and A. I. Plekhanov, Metal-enhanced fluorescence of pseudoisocyanine J-aggregates formed in layer-by-layer assembled films, *J. Phys. Chem. C* **119**, 2743 (2015).

- [33] J. M. Hyman, D. W. McLaughlin, and A. C. Scott, On Davydov's alpha-helix solitons, *Physica D: Nonlin. Phenom.* **3**, 23 (1981).
- [34] Yu. B. Gaididei, K. Ø. Rasmussen, and P. L. Christiansen, Nonlinear excitations in two-dimensional molecular structures with impurities, *Phys. Rev. E* **52**, 2951 (1995).
- [35] J. K. Eilbeck, Reflection of short pulses in linear optics, *J. Phys. A: Math. Gen.* **5**, 1355 (1972).
- [36] L. Allen and J. H. Eberly, *Optical Resonances and Two-level Atoms* (Wiley and Sons, New York, 1975).
- [37] H. Steudel and R. Meinel, Darboux transformations for "W-problems", *Physica D* **87**, 127 (1995).
- [38] D. J. Kaup, The method of solution for stimulated Raman scattering and two-photon propagation, *Physica D: Nonlin. Phenom.* **6**, 143 (1983).
- [39] A. A. Zabolotskii, The quasiself-similar asymptotic of four-wave nondispersive interaction, *Physica D: Nonlin. Phenom.* **40**, 283 (1989).
- [40] L. D. Faddeev and L. A. Takhtajan, *Hamiltonian Methods in the Theory of Solitons*, Classics in Mathematics (Springer, Berlin, 2007), pp. x+592.
- [41] R. F. Bikbaev, A. I. Bobenko, and A. R. Its, Landau-Lifshitz equation, uniaxial anisotropy case: Theory of exact solutions, *Theor. Math. Phys.* **178**, 143 (2014).
- [42] C. M. Bowden and J. P. Dowling, Near-dipole-dipole effects in dense media: Generalized Maxwell-Bloch equations, *Phys. Rev. A* **47**, 1247 (1993).